



ENGINEERING SCIENCES

Advantages of treating sponge-gourd waste by mechanical refining on the properties of fiber-based poly(butylene adipate-co-terephthalate)/polylactide biocomposites

THIAGO R. CORREIA, RENAN HENRIQUES G. ALMEIDA, GUSTAVO N. CAMPOS, CAIO C. SANTOS, MARCOS VINICIUS COLAÇO, MARCO ANTONIO G. FIGUEIREDO, ANA MARIA F. SOUSA & ANA LÚCIA N. SILVA

Abstract: This study compares the morphology, thermal, and dynamic-mechanical properties of composites based on polybutylene adipate terephthalate/polylactide biocomposites with sponge gourd waste treated code as R, and non-treated sponge gourd, coded as NR, by mechanical disc refining after milled process. Extrusion followed by compression molding was used to produce biocomposites with fiber contents of 0, 2.5, 5, 10, and 15% wt/wt for R and NR sponge gourd fibers. Scanning electron microscopy analysis reveals that NR has the morphology of a rigid tubular shape, whereas R is a thinner, twisted, and fibrillated fiber. Regardless of the type of sponge gourd fiber used, the thermal stability of the composite decreases as the sponge gourd content increases. At 25°C, the biocomposite with 10%wt/wt R fiber has the highest storage modulus value. The comparison of Tangent δ peak values reveals that the presence of sponge gourd fibers reduces the energy dissipation of the biocomposites. The analysis of the loss modulus at 25°C reveals that R fiber contributes more to the reduction of energy dissipation of the biocomposites than NR. Furthermore, the Cole-Cole plot shows that R and NR fibers are dispersed and do not significantly change the homogeneity of the biopolymer systems.

Key words: Dynamic-mechanical properties, mechanical disc refining, polybutylene adipate terephthalate, polylactide, sponge gourd waste, thermal degradation.

INTRODUCTION

Product design or redesign requires that the project goes beyond meeting technical and economic specifications; in other words, a sustainability aspect must be incorporated. This approach should consider the use of sustainable feedstocks, the production of sustainable products, and/or the effect of the product on the environment after its end-of-life (Joustra et al. 2021, Ruffino 2021). Lignocellulosic fibers derived from agricultural waste emerges as feedstocks for developing polymer composites due to their

appealing characteristics, such as lightness, mechanical properties, biodegradability, and renewability, which are beneficial for the manufacture of packaging materials (Azman et al. 2021, Gallos et al. 2017, Kannan & Thangaraju 2021, Okolie et al. 2021).

Sponge gourd (or *Luffa cylindrica*) is a cucurbitaceous vegetable grown in several countries throughout the tropics and subtropics. The sponge gourds, which are composed of approximately 60% wt. cellulose, 30% wt. hemicellulose, and 10% wt. lignin in a

dried base, are used to manufacture personal hygiene products, panels, decks, automotive components, and microspunge structures for environmental remediation (Khadir et al. 2021, Psarra & Papanicolaou 2021). However, due to the sponge gourds' winding corners, a significant amount of waste can be generated during the manufacturing of their industrial products, motivating the development of additional research using their scraps in several areas, including polymer composites (Guo et al. 2019, Saraiva et al. 2016).

Sponge gourd fibers are recognized as suitable candidates for reinforcing polymer composites because their Young's modulus (about 2.4 GPa) is comparable to lignin (2.0 GPa) and plant hooks (2.0 - 23.0 GPa) (Chen et al. 2014, Zhang et al. 2021). To achieve better compatibility between the polymer matrix and the fiber, the sponge gourd must be treated to remove contaminants and/or modify the fiber surfaces and morphology (Guo et al. 2019, Khadir et al. 2021, Psarra & Papanicolaou 2021, Saraiva et al. 2016, Zhang et al. 2021). Guo et al. (2019) investigated the mechanical properties of poly(hydroxybutyrate-co-valerate) composites using treated sponge gourd fibers in a solution of 5% NaOH and 5% H₂O₂ (volume ratio of 1:1). The advantages of preparing polyester composites filled with different contents of sponge gourd treated with NaOH, Ca(OH)₂, and silane were compared and discussed by Kalusuraman et al. (2020). Tripathy et al. (2020) found that gamma-irradiating sponge gourd fiber surfaces increased the glass transition temperature and decreased the thermal stability of poly(lactic acid), PLA, as the irradiation dose increased.

Mechanical refining is a common process in the pulp and paper industry that is carried out in refiners. Fibers are subjected to large compression and shear forces in this process, which promote significant structural changes

such as fibrillation, fine formation, fiber shortening, fiber straightening, and changes in crystallinity and distribution of surface chemical composition (Gharehkhani et al. 2015, Park et al. 2016). Kelly et al. (2021) recently published a study that links the fibrillation degree of cellulose and lignocellulose nanofibrils processed by a mechanical refiner to their adhesion behavior in the production of structural composites. Furthermore, mechanical disk refining is being studied alone or in conjunction with other treatment processes to improve biomass cellulose digestibility (Chen et al. 2020, Park et al. 2016, Skinner et al. 2020).

Given the scarcity of research on the use of mechanical refiners for treating lignocellulosic fibers for polymer composite applications, this study investigated the effect of treating sponge gourd waste in a mechanical disc-refiner before using them as fibers in a commercial poly(butylene adipate-co-terephthalate)/ polylacticde (PBAT/PLA) blend. Composites were made with different contents of refined and non-refined sponge gourd fibers, and their thermal degradation and dynamic-mechanical properties were studied. The PBAT/PLA blend was chosen because of its appealing mechanical and biodegradability properties (Hernández-López et al. 2019, Musioł et al. 2018), which contribute to the development of sustainable products. The PBAT, PLA and their blend are identified as having the potential to replace conventional thermoplastics as sustainable alternatives for packing, bags, agricultural films, ultraviolet radiation blockers, and foamed plastic applications (del Campo et al. 2021, Cardoso et al. 2022, Hernández-López et al. 2019).

MATERIALS AND METHODS

Materials

Sponge gourd waste were donated by Co-op, localized in Bonfim City, Minas Gerais, Brazil. A commercial blend of poly(butylene adipate-co-terephthalate)/polylactide (PBAT/PLA) grade Ecovio® F2224 was acquired OEKO Bioplásticos. This blend is composed of approximately 45 wt.% of PLA and 55 wt% of PBAT and presents a density of 1.24–1.26 g.cm⁻³ (ISO 1183) and melt volume flow-rate of 3.0 – 6.5 cm³.10min⁻¹ (190°C/5kg, ISO 1133). Coconut oil, used as aid-process, was acquired in local market.

Sponge gourds treatment

Sponge gourd waste in a scrape shape were cleaned to remove impurities, milled in a mill (Willey Solab, model SL-32), and classified into 20 mesh sieve size Tyler. Then, this milled sponge gourd was separated into two batches. Batch #1 was assigned the code NR (Non-refined). The batch #2 was used to make an aqueous suspension with a consistency of 2.9% wt/wt (weight in grams of oven-dry fiber in 100 g of pulp-water mixture) and pH 12 adjusted with NaOH. After 12 h of resting, this aqueous suspension was processed in a disc-refiner (Regmed MD-300, disk: diameter: 120mm, bar width: 4.6 mm, bar height: 46.4 mm, groove width: 3.5 mm;) for 2 min at 0.1 mm disk-gap. At the end of the time, the sponge gourd suspension was discharged, filtered, dried in a forced-air oven at

50°C for 40 h, manually screened using a Tyler sieve mesh 20, and coded as R (refined).

PBAT/PLA/sponge gourd biocomposites preparation

To investigate the effect of each fiber in the PBAT/PLA, biocomposites were prepared with 2.5, 5, 10, and 15% wt/wt of refined (R) and non-refined (NR) sponge gourd fiber. The experimental code was **AA-BB**, where **AA** represents the fiber type (R or NR) and **BB** represents the amount of fiber (2.5, 5, 10, and 15). All biocomposites contained 2% wt/wt coconut oil (process aid), which was added to bring the fibers and pellets together and prevent them from separating in the feeder during extrusion. Furthermore, PBAT/PLA without sponge gourd fibers used, as a reference, was processed under the same conditions as PBAT/PLA biocomposites, including coconut oil. Table I lists all the formulations used in this study.

The main steps in the biocomposite's preparation were premix, extrusion, and compression molding. First, the amounts of PBAT/PLA (pellet) and sponge gourd fibers in each formulation (Table I) were mechanically mixed for 5 min at 70–100 rpm in a “V” powder mixer (CFW- 10). The PBAT/PLA/R, PBAT/PLA/NR, and neat PBAT/PLA were then dried for 24 h in a forced-air oven at 60°C. Following the drying process, coconut oil was added to each formulation just prior to the extrusion process. The extrusion was carried out in a Tecktril

Table I. Formulation of the PBAT/PLA, PBAT/PLA/R and PBAT/PLA/NR biocomposites (% wt/wt).

Component	PBAT /PLA	R-2.5	R-5	R-10	R-15	NR-2.5	NR-5	NR-10	NR-15
PBAT/PLA	98	95.5	93	88	83	95.5	93	88	83
R	-	2.5	5	10	15	-	-	-	-
NR	-	-	-	-	-	2.5	5	10	15
Coconut Oil	2	2	2	2	2	2	2	2	2

DCT-20 co-rotating twin-screw extruder (L/D ratio of 36), with a screw rotation of 200 rpm, a feed rate of 5 kg.h⁻¹, a temperature set profile of 70/150/165/165/165/165/170°C, and the screw profile shown in Figure 1.

After extrusion, all experiments were pelletized and dried in a forced-air oven at 60°C for 20 h before compression molding. Flat sheets with dimensions of 100mm x 100mm and a thickness of 1 mm were produced using the Carver press model C at 170°C for 3 min under 5 MPa, followed by a cooling step in another Caver press at 5 MPa for 2 min.

Characterization of the biocomposites

Scanning electron and optical microscopies

The morphology of the cryofractured surface of the biocomposites was observed using JEOL JSM-6510LV scanning electron microscope (SEM). The surfaces of the samples were sputter-coated with gold before analysis. Surface photos of PBAT/PLA of the PBAT/PLA/R and PBAT/PLA/NR were recorded using a Nikon SMZ800 stereomicroscope (20 x magnification, 1 μm resolution, sample area of 5.94 x 4.45 mm).

Thermogravimetric analysis

Thermogravimetric analysis (TGA) was carried out in a Q50 series thermogravimetric analyzer, TA Instruments under nitrogen atmosphere, temperature range of 50 to 600°C, heating rate

of 10°C.min⁻¹, and sample amount about 15 mg. The results are expressed as mass loss (TGA) and derivative of mass loss (DTA). From each thermogram, the temperature at 5% of mass loss (T5%) in TGA curve and temperature at the maximum mass loss rate (Tpeak) in DTA curve are reported.

Dynamic-mechanical analysis

Dynamic mechanical analyzer (DMA, TA-Q800) was used to investigate the dynamic-mechanical properties of the biocomposites as a function of temperature. Samples with dimensions of 25mm x 5mm x 1mm were tested in the tensile geometry with oscillation strain of 0.09%, frequency at 1 Hz, temperature ranged from 0 to 100°C, and heating rate of 3°C.min⁻¹. This analysis generated curves of storage modulus (E'), loss (E'') modulus, and tan δ in function of temperature. E' and E'' are related to the ability of a material store and dissipate energy, respectively, and tangent δ (tan δ) is known as damping factor, representing by the ratio of E''/E'.

Data acquisition, plotting and analyzing

The data from TGA and DMA analysis were collected from Trios TA Instruments v.5. All graphics were plotted using the software QtiPlot 0.9.8.3 and drawings were created using ImageJ and Inkscape 1.1.

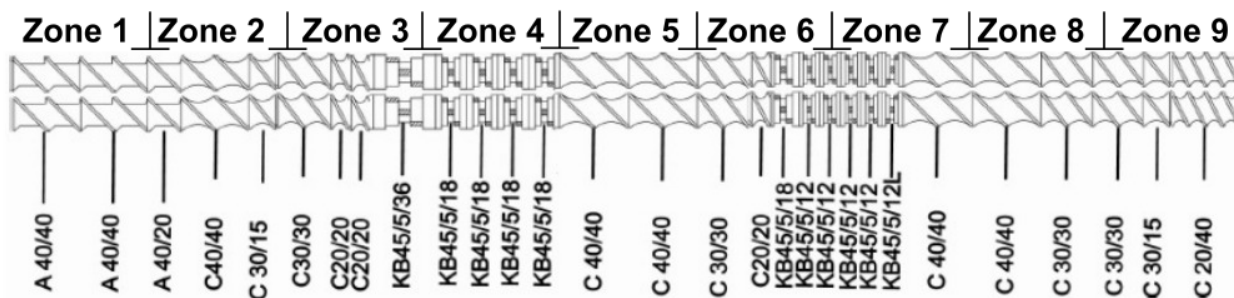


Figure 1. Extruder screw profile.

RESULTS AND DISCUSSION

Morphology

Figure 2 depicts SEM images of the cryofractured surfaces of the biocomposites R-15 (a) and NR-15 (b), as well as the sponge gourds fibers R(c) and NR(d).

The comparison of the photos in Figure 2 shows that there is a significant difference in the morphologies of R (Figure 2a, c) and NR (Figure 2b, d) fibers. Unlike the tubular shape of NR (Figure 2d), the mechanical treatment opens the sponge gourd fibers, separating their bundles and exposing the inner layers of R (Figure 2c) fiber. Furthermore, R fibers (Figure 2c) are more twisted and have a smaller diameter than NR fibers (Figure 2d). This morphological difference suggests that the R fiber has a higher available contact surface area than the NR. Although the literature reports that the extrusion process often generates causes fiber bundle breakage or scission (Gallos et al. 2017), this effect is not observed in this study since the morphologies of the NR and R fibers in the biocomposite (highlighted in the Figures 2a-b) remain the

same as those before the extrusion process (Figure 2c-d).

The morphology of the biocomposites was also investigated using stereo-microscope photos, as shown in Figure 3. The visual analysis of photos reveals that NR fibers are more visible than R fibers, which is reasonable given the higher diameter of NR. Furthermore, the addition of 2.5% and 5% NR fibers to the PBAT/PLA blend appears insufficient to produce a uniform dispersion, as areas with no fibers are visible. The same finding is obtained with PBAT/PLA containing 2.5% R fiber (R-2.5). Furthermore, as the R and NR fiber contents of the PLA/PBAT blend increase, the individual fibers become closer together but without form agglomerates. However, the stereo-micrographs show that R fibers are better dispersed in the PLA/PBAT matrix comparing to NR fibers.

Thermogravimetric analysis

Figure 4 shows the overlay of the thermal degradation curves of PBAT/PLA blend versus R (Figure 4a) and PBAT/PLA blend versus NR

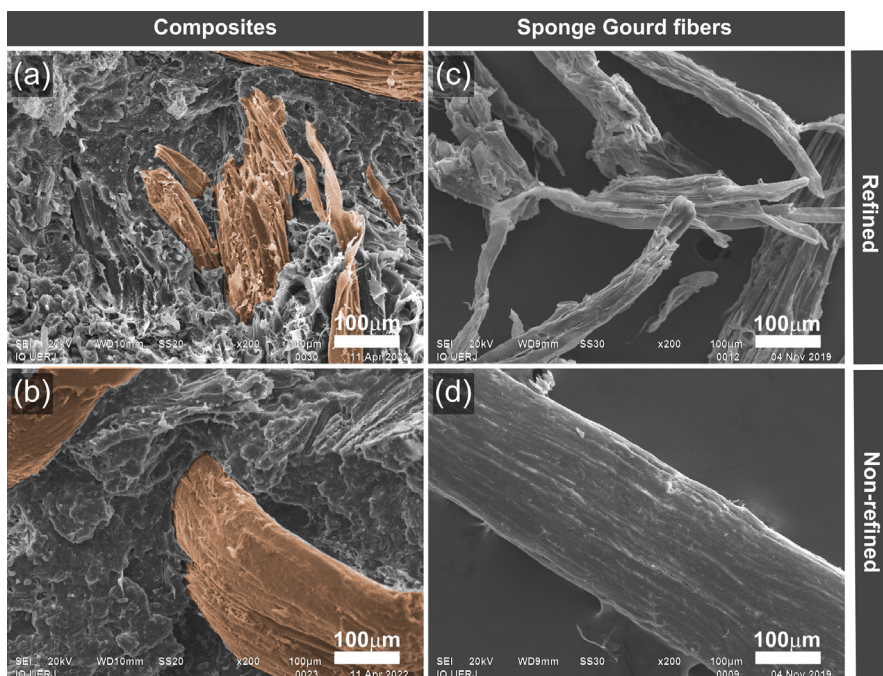


Figure 2. SEM photomicrography (magnification of x200, 100 mm) of (a) biocomposite R-15, (b) biocomposite NR-15, (c) sponge gourd R, and (d) sponge gourd NR. Sponge gourd fibers are highlight in (a) and (b) at RGBA(255,153, 85,100) color using software Inkscape1.1.

(Figure 4b). The degradation temperatures are shown in Table II.

The PBAT/PLA blend (Fig 4a-b, red line) exhibits a two-stage degradation profile related to the PLA and PBAT, respectively. The PBAT/PLA blend contains 52 wt.% of PBAT and 48 wt.% of PLA, which is consistent with manufacturer data. Both R and NR sponge gourd fibers degrade in a single stage (Figure 4a-b, green line). Furthermore, the DTA curve of NR presents a shoulder around 200 – 300°C, whereas R fibers do not. The absence of the shoulder in the DTA curve of R is attributed to the removal of some of its hemicellulose content during mechanical refining (Correia et al. 2021), which contributes to

a higher T5% at around 10°C when compared to the NR curves.

Figure 4c-f depicts the TGA curves of PBAT/PLA/R and PBAT/PLA/NR. The degradation temperatures are shown in Table II. DTA curve comparison (Figure 4c-d) shows that both PBAT/PLA/R and PBAT/PLA/NR have a two-stage degradation, similar to PBAT/PLA blend. Furthermore, Tpeak1 is slightly shifted toward lower temperature values, whereas Tpeak2 localization remains virtually unchanged. T5% is reduced in the same way that Tpeak1 is reduced (Figure 4e-f, Table II). In fact, a comparison of the data in Table II shows that as the content of sponge gourd in the biocomposite increases, the values of Tpeak1 and T5% tend to shift toward lower temperatures, with this reduction being more pronounced for the R-15.

The effect of sponge gourd type and content on T5% and Tmax1 reduction can be attributed to the fact that cellulose, the main constituent of sponge gourd fiber, releases H₂O during thermal decomposition, which contributes to PLA chain scission (Liu et al. 2010, Paajanen & Vaari et al. 2017). Furthermore, the sponge gourd refined fibers have a higher devolatilization index, which was attributed to the increased accessible surface area generated by mechanical refining, implying that the R fiber is more thermal reactive than the NR (Correia et al. 2021). PBAT/PLA filled with office wastepaper fiber showed a similar trend of decreasing thermal stability when compared to the PBAT/PLA blend (Xu et al. 2019).

Dynamic mechanical analysis

The effect of NR and R fibers on the storage modulus (E'), loss modulus (E'') and loss factor ($\tan \delta$) of the biocomposites was assessed by DMA. Figure 5 shows the comparison of temperature dependence of E' for PBAT/PLA

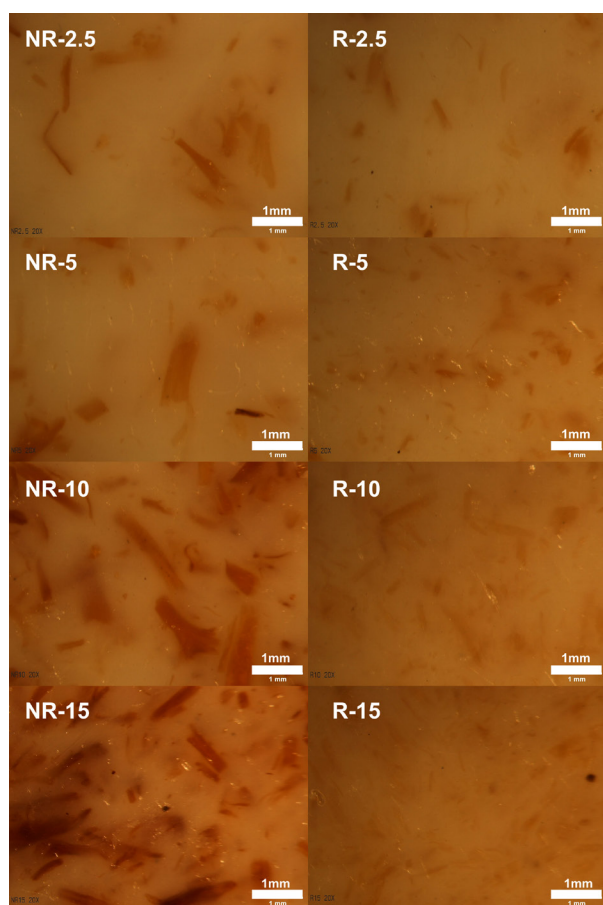


Figure 3. Photos from stereo-microscope (sample area of 5.94 x 4.45 mm²) of PBAT/PLA/sponge gourd biocomposites filled with different content of R fibers (column left) and NR (column right).

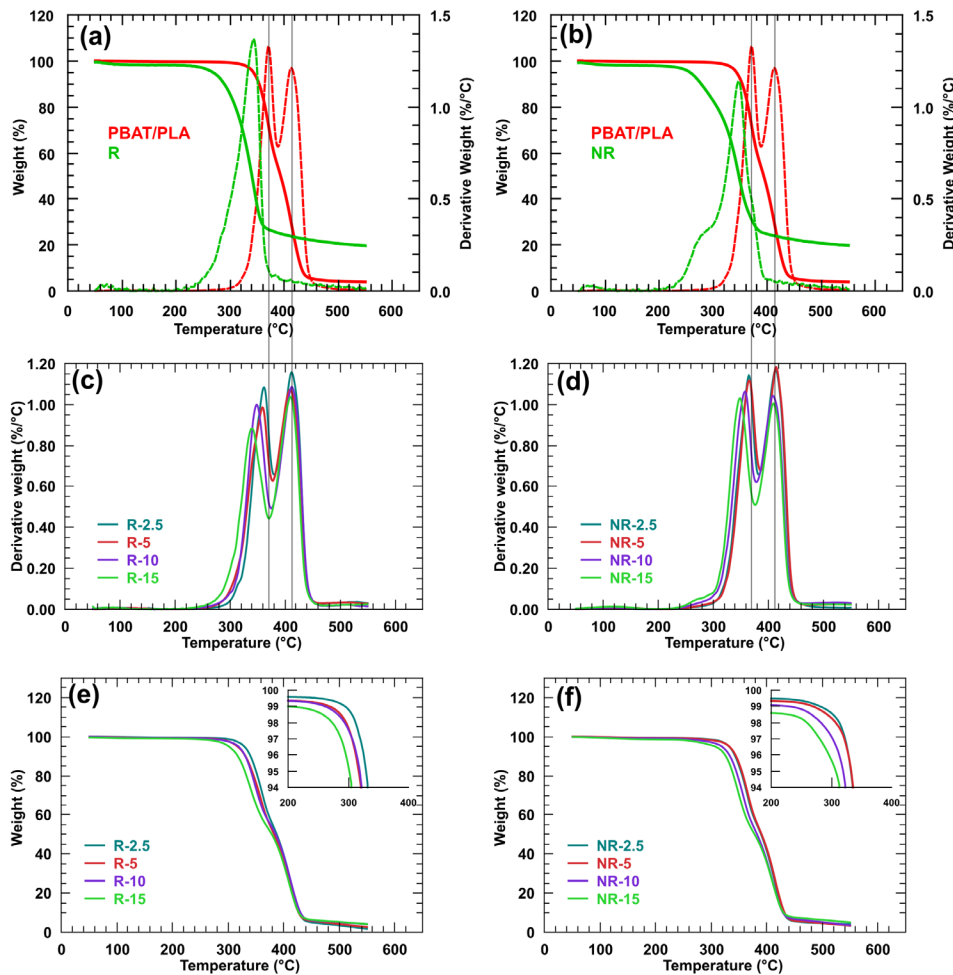


Figure 4. TGA and DTG plots of PBAT/PLA (a and b), R fiber (a), NR fiber (b), and PBAT/PLA biocomposites filled with R fibers (c and e) and NR (d and f).

blend with PBAT/PLA/R (Figure 5a) and PBAT/PLA/NR (Figure 5b).

Similar profiles of the temperature dependence of E' are observed for all materials, as shown in Figure 5. The PBAT/PLA blend and all biocomposites show higher values of E' up to about 50°C, then a sharp decrease in E' due to the increase in the phase of PLA chain mobility (T_g transition) up to a small plateau (in the rubbery region), followed by an increase in E' . The increase in E' in the rubbery region is caused by the cold crystallization of PLA during the test, according to the literature (Arias et al. 2013, Yokesahachart et al. 2021).

In this study, the behavior of E' at temperatures ranging from zero to close to 50°C (marked with yellow box in Figure 5) was

highlighted in particular. This temperature range was chosen based on possible common applications for this type of biocomposite, such as packaging. Figure 5 shows that adding sponge gourd increases E' values, even though this effect does not appear to follow a linear trend with fiber content, regardless of type. Figure 6 plots the values of E' at 25°C among the biocomposites to better evaluate this behavior.

When compared to the PBAT/PLA blend, neither NR-2.5 nor R-2.5 biocomposites improve E' at 25°C. These findings indicate that the content of 2.5% sponge gourd fibers is insufficient to produce any reinforcement, regardless of whether the sponge gourd fiber is treated or not. Furthermore, the amount of sponge gourd that produced the highest values

Table II. Degradation Temperatures from TGA/DTG curves.

Sample Code	Temperature (°C) (±1)		
	T5%	1 st peak of DTA	2 nd peak of DTA
PBAT/PLA	343	371	413
R	266	347	-
NR	257	344	-
PBAT/PLA/R composites			
R-2.5	329	361	412
R-5	317	359	410
R-10	319	348	412
R-15	301	340	410
PBAT/PLA/NR composites			
NR-2.5	332	365	414
NR-5	333	366	414
NR-10	319	358	409
NR-15	307	349	410

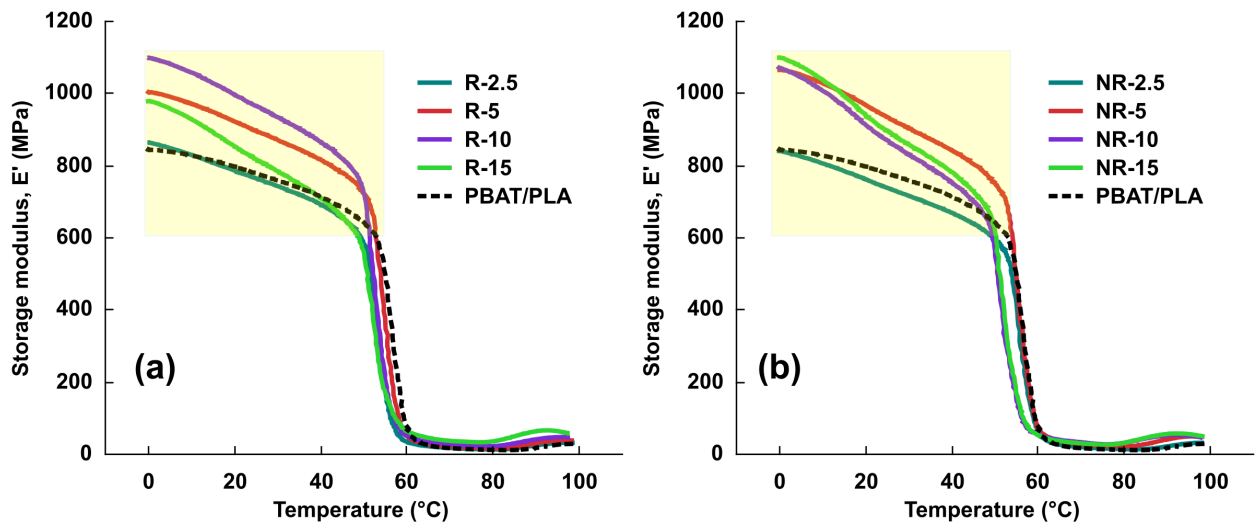


Figure 5. Temperature dependence of storage modulus of PBAT/PLA blend (a and b), PBAT/PLA/R (a), and PBAT/PLA/NR (b).

of E' at 25°C is 10%w/w for R and 5%w/w for NR, resulting in a 24% and 20% improvement in E' over the PBAT/PLA blend, respectively.

The plots of damping factor $\tan \delta$ (ratio of loss modulus to storage modulus, $\tan \delta = E''/E'$) as a function of temperature are shown in Figure 7. Data of the peak of $\tan \delta$ ($\tan \delta_{peak}$) and the glass transition temperature (T_g) related to the

PLA were obtained from the curves in Figure 7 and are reported in Table III.

A reduction in the T_g values is observed for the biocomposites being that mostly pronounced for PBAT/PLA/R. Therefore, based on this analysis, one may infer that the addition of sponge gourd to the PBAT/PLA blend helped increase the polymer mobility, in which R fibers appear to have a higher effect. In contrast,

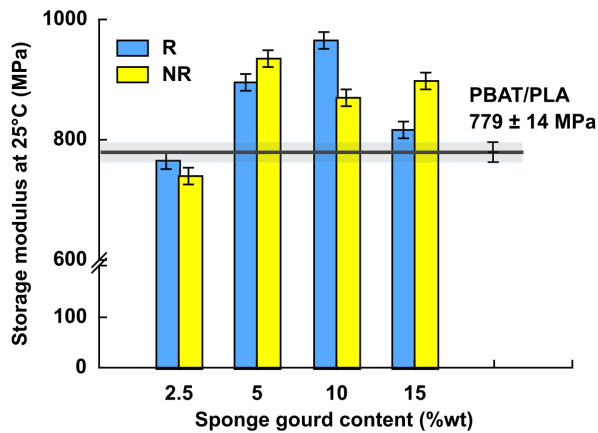


Figure 6. Storage modulus values at 25°C of PBAT/PLA and PBAT/PLA/sponge gourd biocomposites. The gray line represents the average value of E' of PBAT/PLA.

an opposite result can be drawn looking for the values of $T_{\text{and}_{\text{peak}}}$ since all biocomposites showed a trend of reduction with increasing fiber content, comparing to PBAT/PLA matrix. This behavior indicates that sponge gourd cause restrictions to the chain's polymer movement. Furthermore, biocomposites with R fibers tend to have higher $\text{Tan } \delta$ values than NR biocomposites, except the R-15 biocomposite, which presents a lower $\text{Tan } \delta$ value than NR-15, signaling a more pronounced elastic behavior of R-15. A recent review (Bashir 2021) regarding the characterization of filled polymer by DMA

reported that most of the studies showed a relation between the reduction $T_{\text{and}_{\text{peak}}}$ with the existence of strong interfacial interactions of the filler and polymer matrix; nonetheless, the same behavior was not verified for the increase in T_g . Therefore, based on $T_{\text{and}_{\text{peak}}}$ data (Table III) or T_g , one can infer that as more sponge gourd is added to the biocomposite, energy dissipation decreases because the presence of fibers restricts the movement of the polymers, as well as a reduction in the volume PBAT/PLA in the biocomposite.

However, it is important to highlight the that the linear dependence of $T_{\text{and}_{\text{peak}}}$ with sponge gourd load in the biocomposite is more significant for R fiber (R-squared of 92.94%) than the NR one (R-squared of 45.9%). This behavior can be attributed to the thinner and twisted morphology of R fibers, which contributes to produce a tangled structure that help to retain the polymer, compared to the rigid and tubular shape of the NR fiber.

The loss modulus, E'' , is a viscoelastic property related to the material's energy dissipation. It is frequently associated with internal friction caused by movements within the material, the relaxation process, morphological

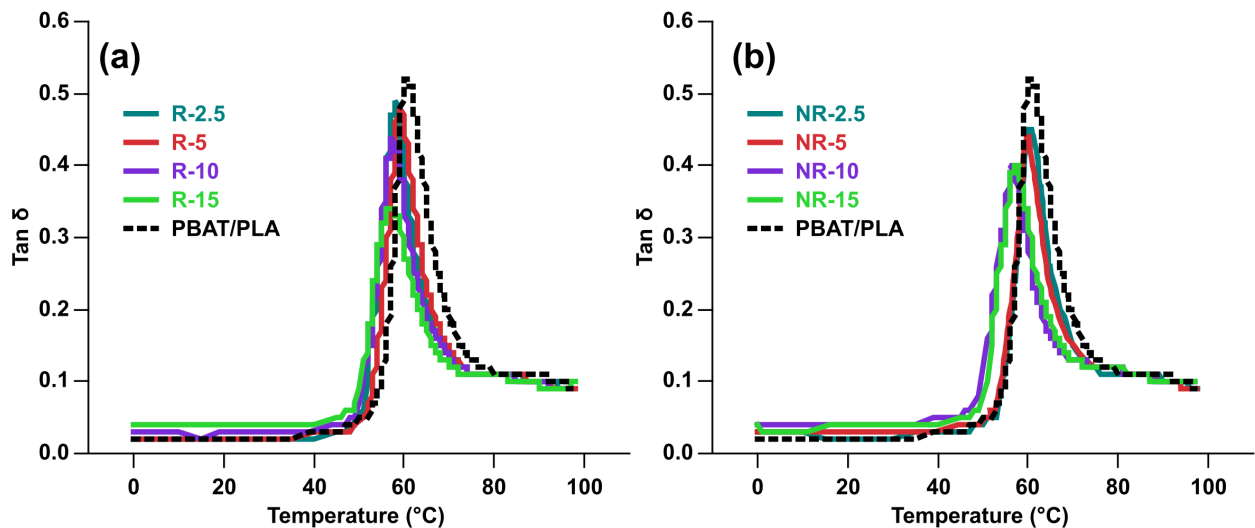


Figure 7. Temperature dependence of $\text{Tan } \delta$ of PBAT/PLA blend (a and b), PBAT/PLA/R (a) and PBAT/PLA/NR (b).

Table III. Tg and Tanδ_{peak} related to the PLA in the PBAT/PLA, PBAT/PLA/R, and PBAT/PLA/NR.

Sample	Tg (°C) ± 0.2	Tanδ _{peak} ± 0.006
PBAT/PLA	60.8	0.520
R-2.5	58.2	0.480
R-5	58.9	0.473
R-10	57.6	0.432
R-15	57.3	0.343
NR-2.5	60.4	0.445
NR-5	58.9	0.401
NR-10	59.7	0.426
NR-15	57.0	0.389

differences, and heterogeneities (Saba et al. 2016). Furthermore, energy dissipation can be also occurred by friction can occur at the interface between fibers, within the fiber bundle, and within the fiber wall, according to Liu et al. (2021). Therefore, based on the preceding statements, it was already expected to observe differences in E'' behavior as a function of fiber type and content. As shown in Figure 8, the addition of sponge gourd fibers raises the E'' values at temperatures ranging from zero to close to 50°C, with this behavior being more

pronounced in biocomposites filled with NR fibers. One explanation for this behavior is that R fiber appears to be more flexible, thinner, and twisted, whereas NR appears to be more rigid, thicker, and packed; thus, it is reasonable to expect NR to produce a higher level of friction than R.

The Cole-Cole plot can be used to investigate the degree of homogeneity in the polymer system. The representation of this plot in perfect semi-circular arc characterizes a homogenous polymer system, whereas any deviation from the semi-circular arc to irregular shapes represents a heterogeneous dispersion (Bommegowda et al. 2021). Figure 9 presents the Cole-Cole plot of PBAT/PLA blend, and PBAT/PLA/R and PLAT/PLA/NR biocomposites. In general, PBAT/PLA/R and PBAT/PLA/NR have very similar semi-circular arcs in Cole-Cole plots to PBAT/PLA, indicating that R and NR fibers are dispersed and do not significantly change the homogeneity of the polymer systems. From the composition with 5 wt.% of fibers (R or NR), more rigid materials are produced compared to the PLA/PBAT matrix. Furthermore, it is possible to observe that PBAT/PLA/R biocomposites tend to have more flexible behavior comparing to PBAT/

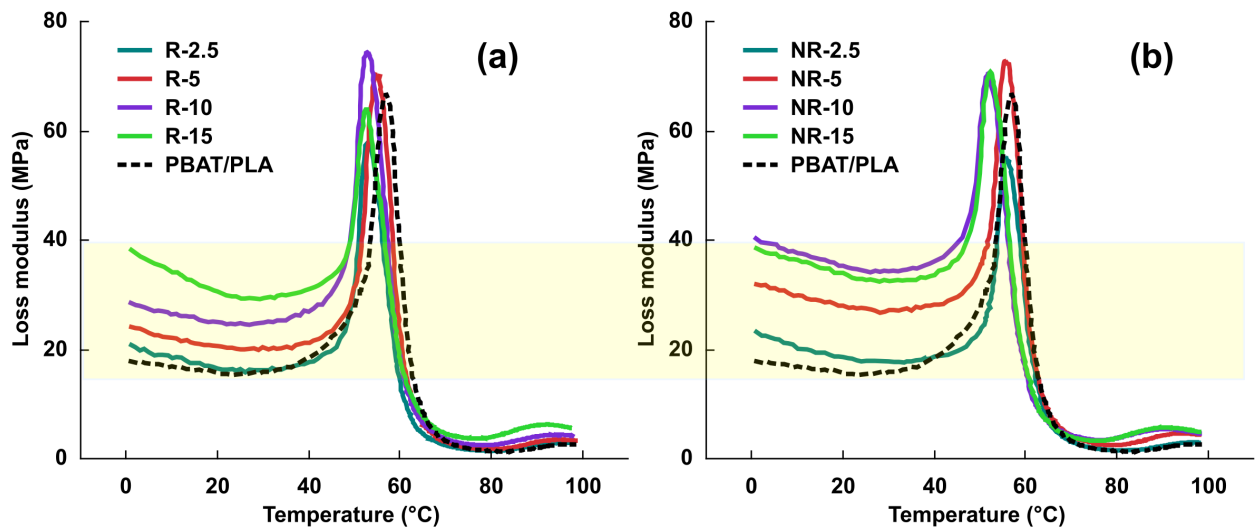


Figure 8. Temperature dependence of E'': (a) PBAT/PLA and PBAT/PLA/R and (b) PBAT/PLA and PBAT/PLA/NR biocomposites.

PLA/NR compositions for longer relaxation times. This behavior agrees with the stereo-micrograph results.

CONCLUSIONS

The impact of using sponge gourd fiber treated (R) and untreated (NR) in a mechanical disc-refiner, as well as their content, on the properties of PBAT/PLA biocomposites was investigated in this study. The refining process altered the morphology of the R fiber, separating their bundles in such a way that the inner layers remained visible, producing fibers with morphology that differed significantly from the tubular shape of non-refined NR fiber.

TGA analysis revealed that the addition of sponge gourd fiber reduced T5% and Tpeak1 temperatures while having no effect on Tpeak2. Tpeak1 was reduced due to water released from

the cellulose during thermal decomposition, which aided in the scission of PLA chains.

The DMA investigation was useful in understanding how the morphology differences between the R and NR affect the viscoelastic properties of the PBAT/PLA/sponge gourd biocomposites. The highest values of E' at 25°C were found for PBAT/PLA blends filled with 10%wt/wt R and 5%wt/wt NR, respectively. Lower Tan δ_{peak} values were observed as more sponge gourd fibers, regardless of type, were added to PBAT/PLA blends, indicating that the fibers reduce the energy dissipation of the blends. Lower loss modulus values were observed for biocomposites with R fibers at temperatures ranging from zero to near 50°C, indicating that the R fiber morphology contributes to reducing energy dissipation of the PBAT/PLA when compared to biocomposites with NR fibers. Furthermore, the Cole-Cole plots show PLA/PBAT/fibers biocomposites present an elastic

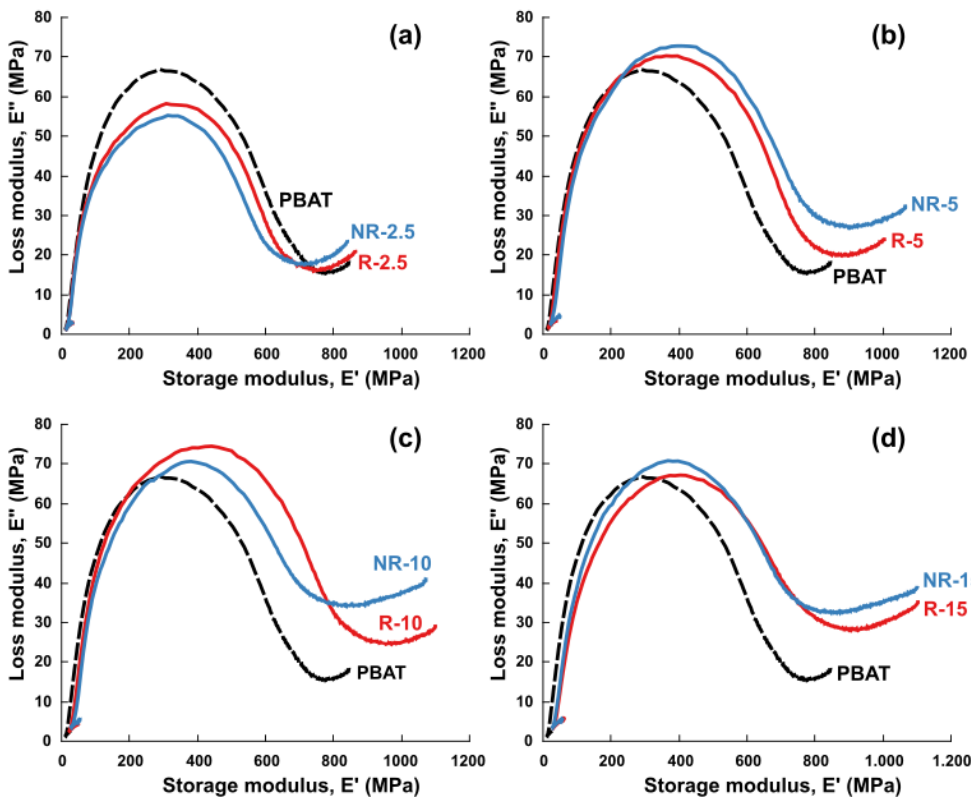


Figure 9. Cole-Cole plot: (a) PBAT/PLA, (b) PBAT/PLA/R and PBAT/PLA/NR composites with 5 %wt. of fibers, (c) PBAT/PLA/R and PBAT/PLA/NR composites with 10 wt.% of fibers and (d) PBAT/PLA/R and PBAT/PLA/NR biocomposites with 15 wt.% of fibers.

behavior more pronounced than PLA/PBAT matrix and that PBAT/PLA/R biocomposites have more flexible behavior comparing to PBAT/PLA/NR compositions for longer relaxation times. Finally, this study demonstrated that using a mechanical disc-refiner is beneficial for treating lignocellulose fibers, changing their properties, and making them a more appealing feedstock for biocomposite production.

Acknowledgments

The authors thank Teadit for making the use of their disc-refiner pilot plant available. The authors acknowledge the Conselho Nacional de Desenvolvimento Científico e Tecnológico – CNPq (309461/2021-9), Fundação de Amparo à Pesquisa do Estado do Rio de Janeiro – FAPERJ (E-26/010.002212/2019 and E-26/010.001927/2019), and Coordenação de Aperfeiçoamento de Pessoal de Nível Superior – CAPES (Financing code 001) for research supporting.

REFERENCES

- ARIAS A, HEUZEY MC & HUNEULT MA. 2013. Thermomechanical and crystallization behavior of polylactide-based flax fiber biocomposites. *Cellulose* 20(1): 439-452.
- AZMAN MA, ASYRAF MRM, KHALINA A, PETRŮ M, RUZAIDI CM, SAPUAN S M, WAN NIK WB, ISHAK MR, ILYAS RA & SURIANI MJ. 2021. Natural fiber reinforced composite material for product design: A short review. *Polymers* 13(12): 1917.
- BASHIR MA. 2021. Use of dynamic mechanical analysis (DMA) for characterizing interfacial interactions in filled polymers. *Solids* 2(1): 108-120.
- BOMMEGOWDA KB, RENUKAPPA NM & RAJAN JS. 2021. Effect of micro-and nanofiller hybrids on the dynamic mechanical properties of glass reinforced epoxy composites. *Polym Compos* 42(5): 2252-2267.
- CARDOSO LG, SILVA J, SILVA JA, CAMILLOTO GP, SOUZA CO, DRUZIAN JI & GUIMARAES AG. 2022. Development and characterization of antioxidant and antimicrobial poly (butylene adipate-co-terephthalate)(PBAT) film incorporated with oregano essential oil and applied in sliced mozzarella cheese. *An Acad Bras Cienc* 94: e20200142.
- CHEN J, ADJALLÉ K, LAI TT, BARNABÉ S, PERRIER M & PARIS J. 2020. Effect of mechanical pretreatment for enzymatic hydrolysis of woody residues, corn Stover and alfalfa. *Waste Biomass Valor* 11(11): 5847-5856.
- CHEN Q, SHI Q, GORB SN & LI Z. 2014. A multiscale study on the structural and mechanical properties of the luffa sponge from *Luffa cylindrica* plant. *J Biomech* 47(6): 1332-1339.
- CORREIA TR, BARROS JPA, SANTOS CC, ESCOCIO VA, LEITE MCA, DE SOUSA AMF & COLAÇO MV. 2021. Characterization of sponge-gourd residue pretreated by mechanical disc refining. *Cell Chem Technol* 55(1-2): 149-157.
- DEL CAMPO A, DE LUCAS-GIL E, RUBIO-MARCOS F, ARRIETA MP, FERNÁNDEZ-GARCÍA M, FERNÁNDEZ JF & MUÑOZ-BONILLA A. 2021. Accelerated disintegration of compostable Ecovio polymer by using ZnO particles as filler. *Polym Degrad Stab* 185: 109501.
- GALLOS A, PAËS G, ALLAIS F & BEAUGRAND J. 2017. Lignocellulosic fibers: a critical review of the extrusion process for enhancement of the properties of natural fiber composites. *RSC Adv* 7(55): 34638-34654.
- GHAREKHANI S, SADEGHINEZHAD E, KAZI SN, YARMAND H, BADARUDIN A, SAFAEI MR & ZUBIR MNM. 2015. Basic effects of pulp refining on fiber properties—A review. *Carbohydr Polym* 115: 785-803.
- GUO Y, WANG L, CHEN Y, LUO P & CHEN T. 2019. Properties of luffa fiber reinforced PHBV biodegradable composites. *Polymers* 11(11): 1765.
- HERNÁNDEZ-LÓPEZ M, CORREA-PACHECO ZN, BAUTISTA-BAÑOS S, ZAVALA-AVEJAR L, BENÍTEZ-JIMÉNEZ JJ, SABINO-GUTIÉRREZ MA & ORTEGA-GUDIÑO P. 2019. Bio-based composite fibers from pine essential oil and PBAT/PLA polymer blend. Morphological, physicochemical, thermal and mechanical characterization. *Mater Chem Phys* 234: 345-353.
- JOUSTRA J, FLIPSEN B & BALKENENDE R. 2021. Circular design of composite products: A framework based on insights from literature and industry. *Sustainability* 13(13): 7223.
- KALUSURAMAN G, SIVA I, MUNDE Y, SELVAN CP, KUMAR SA & AMICO SC. 2020. Dynamic-mechanical properties as a function of luffa fibre content and adhesion in a polyester composite. *Polym Test* 87: 106538.
- KANNAN G & THANGARAJU R. 2021. Recent Progress on Natural Lignocellulosic Fiber Reinforced Polymer Composites: A Review. *J Nat Fibers* 2021: 1-32.
- KELLY PV, GARDNER DJ & GRAMLICH WM. 2021. Optimizing lignocellulosic nanofibril dimensions and morphology by mechanical refining for enhanced adhesion. *Carbohydr Polym* 273: 118566.
- KHADIR A, MOTAMEDI M, PAKZAD E, SILLANPÄÄ M & MAHAJAN S. 2021. The prospective utilization of *Luffa* fibres as a lignocellulosic bio-material for environmental

remediation of aqueous media: a review. *J Environ Chem Eng* 9(1): 104691.

LIU T, BUTAUD P, PLACET V & OUISSE M. 2021. Damping behavior of plant fiber composites: A review. *Compos Struct* 275: 114392.

LIU X, KHOR S, PETINAKIS E, YU L, SIMON G, DEAN K & BATEMAN S. 2010. Effects of hydrophilic fillers on the thermal degradation of poly (lactic acid). *Thermochim Acta* 509(1-2): 147-151.

MUSIOŁ M, SIKORSKA W, JANECEK H, WAŁACH W, HERCOG A, JOHNSTON B & RYDZ J. 2018. (Bio)degradable polymeric materials for a sustainable future–part 1. Organic recycling of PBAT/PLA blends in the form of prototype packages with long shelf-life. *Waste Manag* 77: 447-454.

OKOLIE JA, NANDA S, DALAI AK & KOZINSKI JA. 2021. Chemistry and specialty industrial applications of lignocellulosic biomass. *Waste Biomass Valorization* 12(5): 2145-2169.

PAAJANEN A & VAARI J. 2017. High-temperature decomposition of the cellulose molecule: a stochastic molecular dynamics study. *Cellulose* 24(7): 2713-2725.

PARK J, JONES B, KOO B, CHEN X, TUCKER M, YU JH, PSCHORN T, VENDITTI R & PARK S. 2016. Use of mechanical refining to improve the production of low-cost sugars from lignocellulosic biomass. *Bioresour Technol* 199: 59-67.

PSARRA E & PAPANICOLAOU GC. 2021. Luffa *Cylindrica* as a durable biofiber reinforcement for epoxy systems. *Compos Sci Technol* 203: 108597.

RUFFINO R. 2021. Sustainable design: Aspects of sustainable product development. *BioResources* 16(4): 6548.

SABA N, JAWAID M, ALOTHMAN OY & PARIDAH MT. 2016. A review on dynamic mechanical properties of natural fibre reinforced polymer composites. *Constr Build Mater* 106: 149-159.

SARAIVA AB, PACHECO EB, GOMES GM, VISCONTE LL, BERNARDO CA, SIMOES CL & SOARES AG. 2016. Comparative lifecycle assessment of mango packaging made from a polyethylene/natural fiber-composite and from cardboard material. *J Clean Prod* 139: 1168-1180.

SKINNER C, BAKER P, TOMKINSON J, RICHARDS D & CHARLTON A. 2020. Pressurised disc refining of wheat straw as a pre-treatment approach for agricultural residues: A preliminary assessment of energy consumption and fibre composition. *Bioresour Technol* 304: 122976.

TRIPATHY S, JALI P, PARIDA C & PRADHAN C. 2020. Study on biodegradability and thermal behaviour of composites

using poly lactic acid and gamma-irradiated fibres of *Luffa cylindrica*. *Chemosphere* 261: 127684.

YOKESAHACHART C, YOKSAN R, KHANOONKON N, MOHANTY A K & MISRA M. 2021. Effect of jute fibers on morphological characteristics and properties of thermoplastic starch/biodegradable polyester blend. *Cellulose* 28(9): 5513-5530.

XU C, ZHANG X, JIN X, NIE S & YANG R. 2019. Study on mechanical and thermal properties of poly (lactic acid)/poly (butylene adipate-co-terephthalate)/office wastepaper fiber biodegradable composites. *J Polym Environ* 27(6): 1273-1284.

ZHANG K, WENG B, CHENG D, GUO Y, CHEN T, WANG L, WANG C, XU R & CHEN Y. 2021. Influence of chemical treatment and drying method on the properties of cellulose fibers of luffa sponge. *Int J Biol Macromol* 180: 112-120.

How to cite

CORREIA TR, ALMEIDA RHG, CAMPOS GN, SANTOS CC, COLAÇO MV, FIGUEIREDO MAG, SOUSA AMF & SILVA ALN. 2023. Advantages of treating sponge-gourd waste by mechanical refining on the properties of fiber-based poly(butylene adipate-co-terephthalate)/polylactide biocomposites. *An Acad Bras Cienc* 95: e20230003. DOI: 10.1590/0001-3765202320230003.

*Manuscript received on January 2, 2023;
accepted for publication on February 25, 2023*

THIAGO R. CORREIA¹

<https://orcid.org/0000-0002-0875-9965>

RENAN HENRIQUES G. ALMEIDA³

<https://orcid.org/0000-0003-1393-4366>

GUSTAVO N. CAMPOS¹

<https://orcid.org/0000-0001-9637-0927>

CAIO C. SANTOS¹

<https://orcid.org/0000-0002-1744-704X>

MARCOS VINICIUS COLAÇO²

<https://orcid.org/0000-0002-0174-3063>

MARCO ANTONIO G. FIGUEIREDO¹

<https://orcid.org/0000-0002-3592-7151>

ANA MARIA F. SOUSA¹

<https://orcid.org/0000-0002-4161-3482>

ANA LÚCIA N. SILVA^{3,4}

<https://orcid.org/0000-0002-7668-2576>

¹Universidade do Estado do Rio de Janeiro, Instituto de Química, Rua São Francisco Xavier, 524, Pavilhão Haroldo Lisboa da Cunha, Maracanã, 20550-900 Rio de Janeiro, RJ, Brazil

²Universidade do Estado do Rio de Janeiro, Instituto de Física, Rua São Francisco Xavier, 524, Bloco B, Maracanã, 20550-900 Rio de Janeiro, RJ, Brazil

³Universidade Federal do Rio de Janeiro, Instituto de Macromoléculas Professora Eloisa Mano, Avenida Horácio Macedo, 2013, Bloco J, Cidade Universitária, 21941-598 Rio de Janeiro, RJ, Brazil

⁴Programa de Engenharia Ambiental, Universidade Federal do Rio de Janeiro, Avenida Horácio Macedo, 2013, Bloco J, Cidade Universitária, 21941-598 Rio de Janeiro, RJ, Brazil

Correspondence to: **Ana Maria Furtado de Sousa**

E-mail: ana.furtado.sousa@gmail.com

Author contributions

Thiago Ramos Correia: Methodology, investigation, formal analysis, data curation, and writing-original draft. Renan Henriques Gonçalves de Almeida and Caio Cler dos Santos: Investigation. Gustavo Ninho Campos: Dynamic-mechanical data acquisition and interpretation. Marco Antonio Gaya Figueiredo: Dynamic-mechanical analysis resources. Marcos Vinicius Colaço: Conceptualization, supervision, and writing-review. Ana Maria Furtado de Sousa: Funding acquisition, conceptualization, supervision, and writing—review. Ana Lúcia Nazarethda Silva: Dynamic mechanical analysis validation and final writing-review.

